

Electronic Supplementary Information

Construction of a phos-tag-directed self-assembled fluorescent magnetobiosensor for simultaneous detection of multiple protein kinases

Su Jiang,^{‡a} Yi-xuan Geng,^{‡a} Wen-jing Liu,^{‡b} Zi-yue Wang,^a Chun-yang Zhang ^{*a}

^a College of Chemistry, Chemical Engineering and Materials Science, Shandong Normal University, Jinan 250014, China.

^b School of Chemistry and Chemical Engineering, Southeast University, Nanjing 211189, China.

[‡] These authors contributed equally.

* Corresponding authors: Tel.: +86 0531-86186033; Fax: +86 0531-82615258. cyzhang@sdsu.edu.cn

1. Chemicals and materials

The cAMP-dependent protein kinase (PKA), streptavidin magnetic beads (1 μ m), and ATP were purchased from New England Biolabs, Inc. (Massachusetts, U.S.A.). The RAC α -serine/threonine protein kinase (AKT1) was obtained from Sigma-Aldrich Co (St. Louis, MO, USA). The biotinylated Phos-tag BTL-105 and Phos-tag BTL-111 were bought from Wako Pure Chemical Industries, Ltd (Osaka, Japan). FITC-labeled peptide (FITC-CLRRASLG) and Cy5-labeled peptide (Cy5-CKRPRAASFAE) were obtained from Chinese Peptide Company (Hangzhou, China). 3-isobutyl-1-methylxanthine (IBMX), forskolin (Fsk), phenylmethanesulfonyl fluoride (PMSF), H-89 (N-[2-(p-bromocinnamylamino) ethyl]-5-isoquinolinesulfonamide dihydrochloride) and oridonin (20-epoxy-1- α ,6- β ,7,14-tetrahydroxy-7- α -(14r)-kaur-16-en-15-on) were obtained from Med Chem Express (MCE, USA). Fetal bovine serum (FBS), RIPA Lysis kit, and protein assay kit were obtained from Sangon Biotech (Shanghai, China). Human cervical carcinoma cell line (HeLa cells) and colorectal cancer cell line (HCT-116 cells) were purchased from Cell Bank, Shanghai Institutes for Biological Sciences, Chinese Academy of Sciences (Shanghai, China). All other chemicals were of analytical grade and obtained from Sigma-Aldrich (St. Louis, MO, USA). The ultrapure water was prepared by Millipore filtration system (Millipore, Milford, MA, USA) in the experiments.

2. Imaging of the MB-peptides-FITC/Cy5 nanostructures

The MB-peptides-FITC/Cy5 nanostructures were imaged by the inverted Olympus IX-71 microscope (Olympus, Tokyo, Japan). The fluorescence images of FITC were obtained in green channel with 488 nm excitation, and fluorescence images of Cy5 were obtained in red channel with 640 nm excitation. The photons were collected by an oil immersion 60 \times objective (Olympus, Japan) and imaged onto the two

halves of an Andor Ixon DU897 EMCCD camera (Andor, Belfast, UK) with an exposure time of 100 ms.

For data analysis, regions of interest of 300×300 pixels were selected and analyzed by Image J software.

3. Gel electrophoresis

The formation of the MB-peptides-FITC/Cy5 nanostructures were analyzed by 2 % agarose gel (2.8 g of agarose, 140 mL of $1 \times$ TAE buffer) at 110 V for 50 min. The nanostructures were analyzed by using an illumination source of Epi-blue (460 – 490 nm excitation) and a 516 – 544 nm filter for FITC fluorophores, an illumination source of Epi-red (625 – 650 nm excitation) and a 675 – 725 nm filter for Cy5 fluorophores.

4. Metal ion specificity of phos-tag

To investigate the metal ion specificity of phos-tag in this assay, we replaced Zn^{2+} with four irrelevant metal ions including Mg^{2+} , Cu^{2+} , Fe^{2+} , and Pd^{2+} . After the phosphorylation reaction, 2 μL of $10 \times$ phos-tag reaction buffer (20 mM tris-HCl, 1 M NaCl, 1% tween-20, pH 7.0), 0.4 mM irrelevant metal ions, 2 μL of 20 μM phos-tag, and 6 μL of H_2O were added into the phosphorylation reaction solution, and incubated at 37 °C for 60 min. The protein kinase assay was carried out as described above.

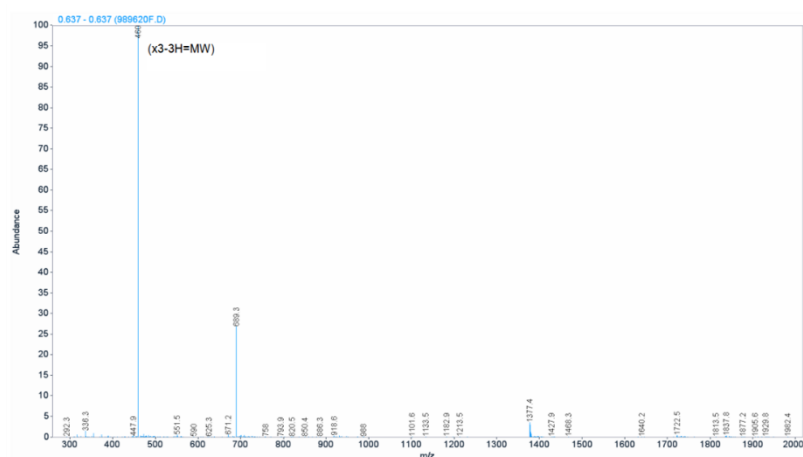
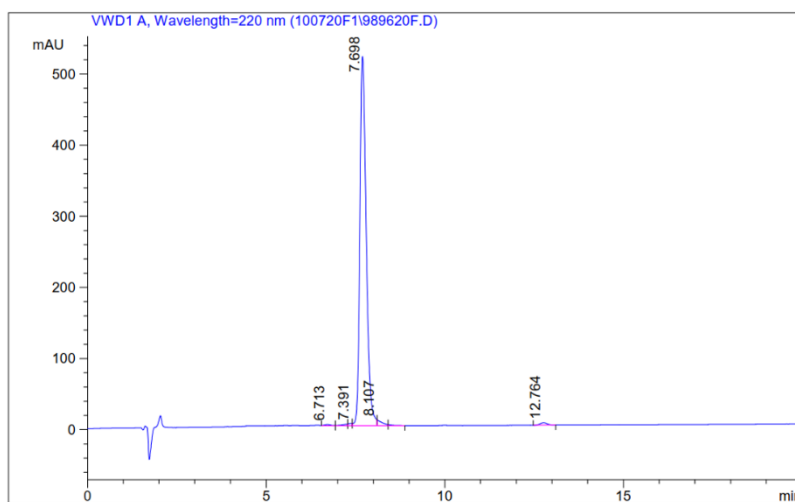
A**B**

Fig. S1. Mass spectral (A) and HPLC (B) analysis of the FITC-peptide substrate. The calculated molecular weight of the peptide substrate is 1377.6 with a peptide purity of 97.0 %.

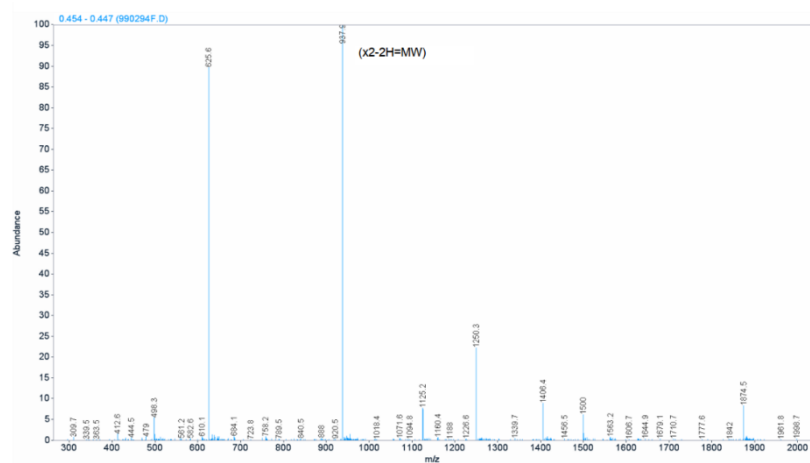
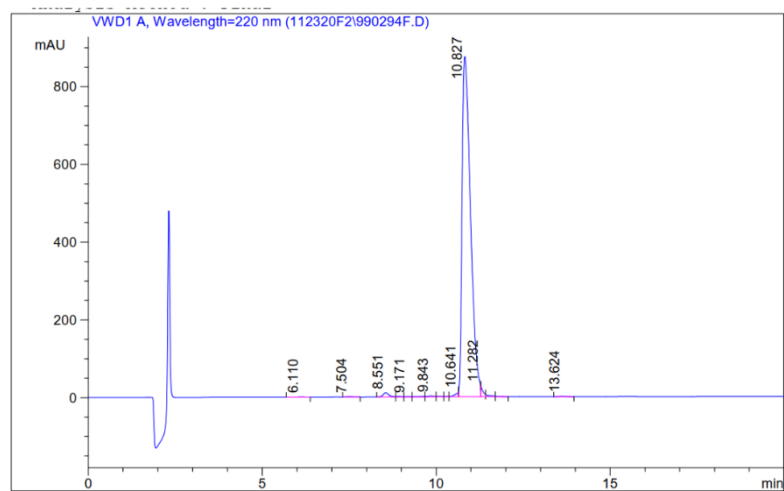
A**B**

Fig. S2. Mass spectral (A) and HPLC (B) analysis of the Cy5-peptide substrate. The calculated molecular weight of the peptide substrate is 1874.2 with a peptide purity of 96.9 %.

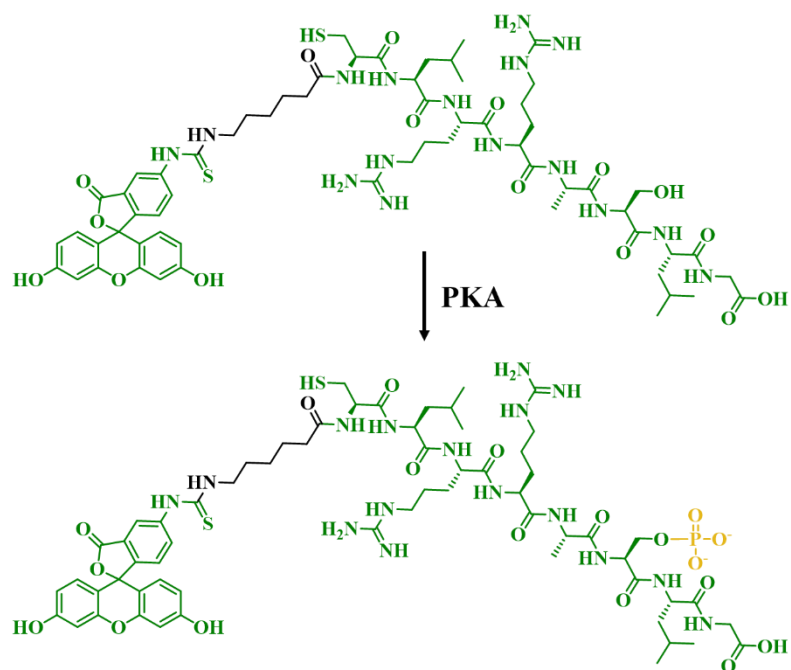


Fig. S3. Mechanism of PKA-mediated phosphorylation of the FITC-peptide substrate. PKA can transfer the γ -phosphate from ATP to serine hydroxyl group of FITC-peptide. The linker between the peptide and FITC is marked in black color. Phosphate group is marked in yellow color.

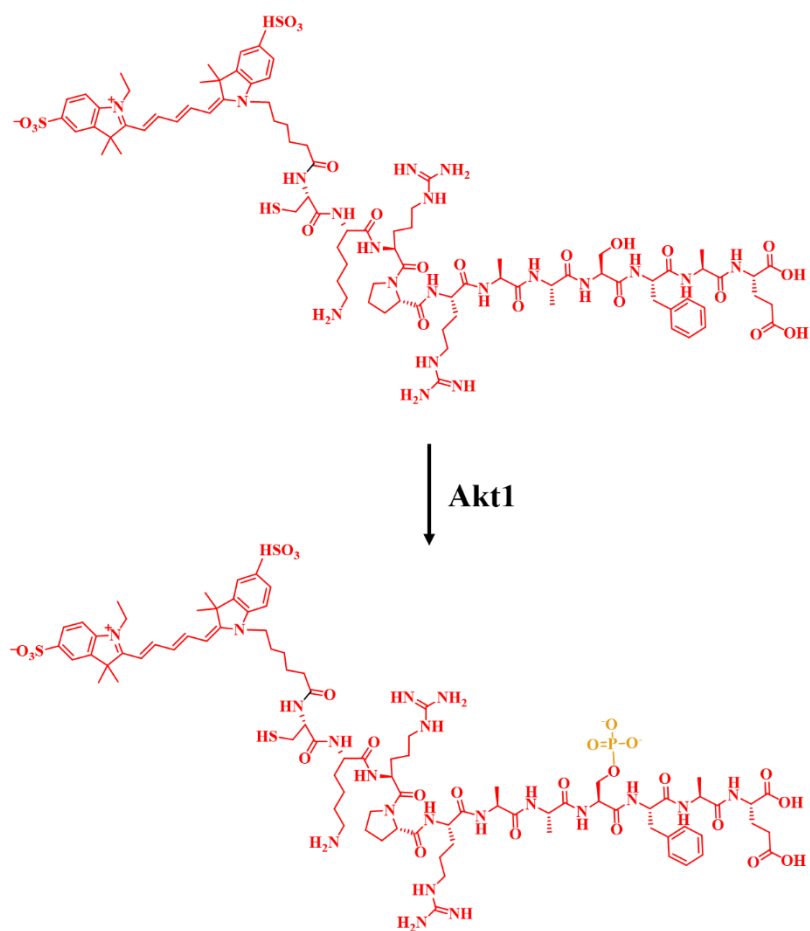


Fig. S4. Mechanism of Akt1-mediated phosphorylation of the Cy5-peptide substrate. Akt1 can transfer the γ -phosphate from ATP to serine hydroxyl group of Cy5-peptide. The linker between the peptide and Cy5 is marked in black color. Phosphate group is marked in yellow color.

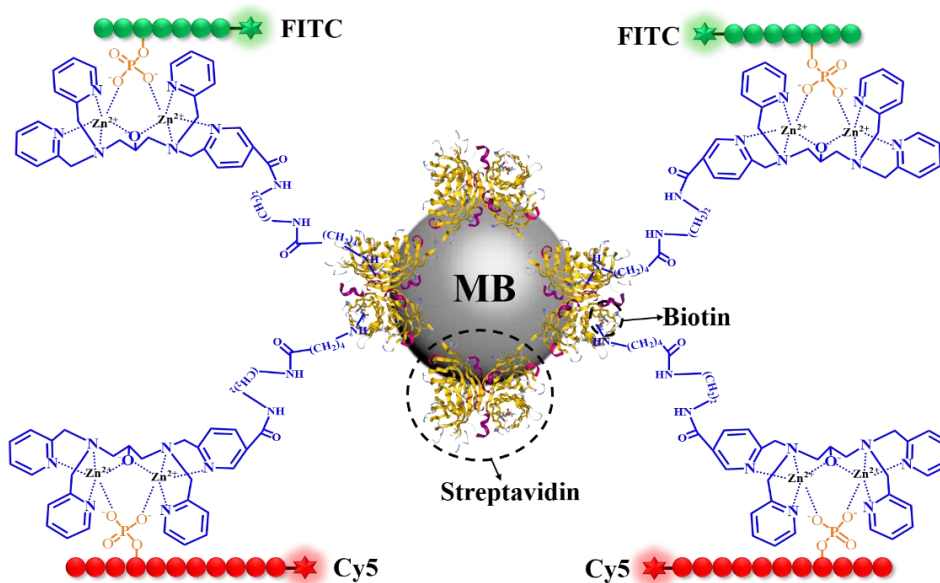


Fig. S5. The detailed structure of the MB-peptides-FITC/Cy5 nanostructure.

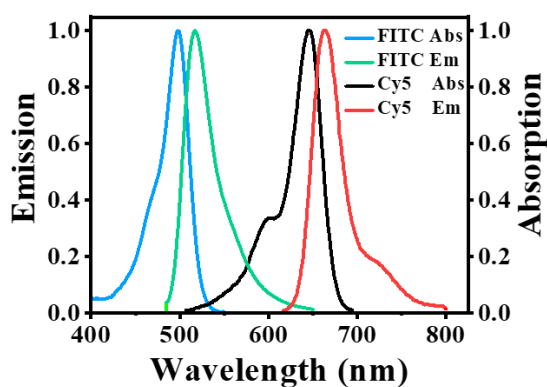


Fig. S6. Normalized absorption and emission spectra of FITC and Cy5. Blue line: absorption spectrum of FITC, green line: emission spectrum of FITC, black line: absorption spectrum of Cy5, red line: emission spectrum of Cy5.

5. Photos of the MB-peptides-FITC nanostructure by 2% agarose gel electrophoresis under white light.

We performed 2% agarose gel electrophoresis to verify the formation of the MB-peptides-FITC/Cy5 nanostructures. As shown in Fig. S7, no migration is observed for both MB-peptides-FITC nanostructure (Fig. S7A) and MB-peptides-Cy5 nanostructure (Fig. S7B) because the particle size of magnetic bead is larger than the pore size of agarose gel.^{1,2}

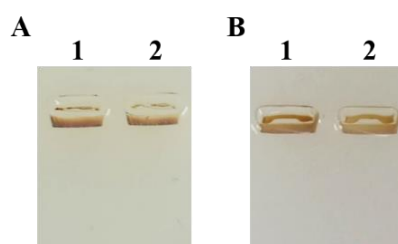


Fig. S7. (A) Photos of the MB-peptides-FITC nanostructure by 2% agarose gel electrophoresis under white light. Lane 1, with 1 U/ μ L PKA; lane 2, without PKA. (B) Photos of the MB-peptides-Cy5 nanostructure by 2% agarose gel electrophoresis under white light. Lane 1, with 10 nM Akt1; lane 2, without Akt1.

6. Fluorescence imaging of the MB-peptides-FITC/Cy5 nanostructures

When PKA is present, only FITC fluorescence signals are generated (Fig. S8A), but no Cy5 fluorescence signal is detected (Fig. S8B). When Akt1 is present, only Cy5 fluorescence signals are generated (Fig. S8E), but no FITC fluorescence signal is detected (Fig. S8D). Moreover, when both PKA and Akt1 are present, both FITC (Fig. S8G) and Cy5 (Fig. S8H) fluorescence signals are detected simultaneously, with yellow color indicating perfect colocalization in the overlay channel (Fig. S8I, yellow color). These results clearly demonstrate that the successful construction of the MB-peptides-FITC/Cy5 nanostructures enable the detection of multiple protein kinases.

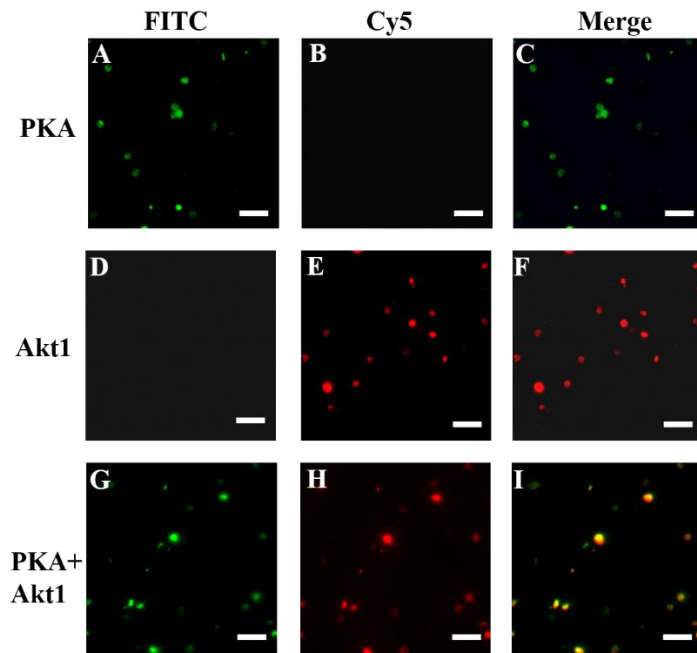


Fig. S8. Imaging of the MB-peptides-FITC/Cy5 nanostructures with an oil immersion $60\times$ objective. The FITC fluorescence signal is shown in green, and the Cy5 fluorescence signal is shown in red. The scale bar is 5 μm .

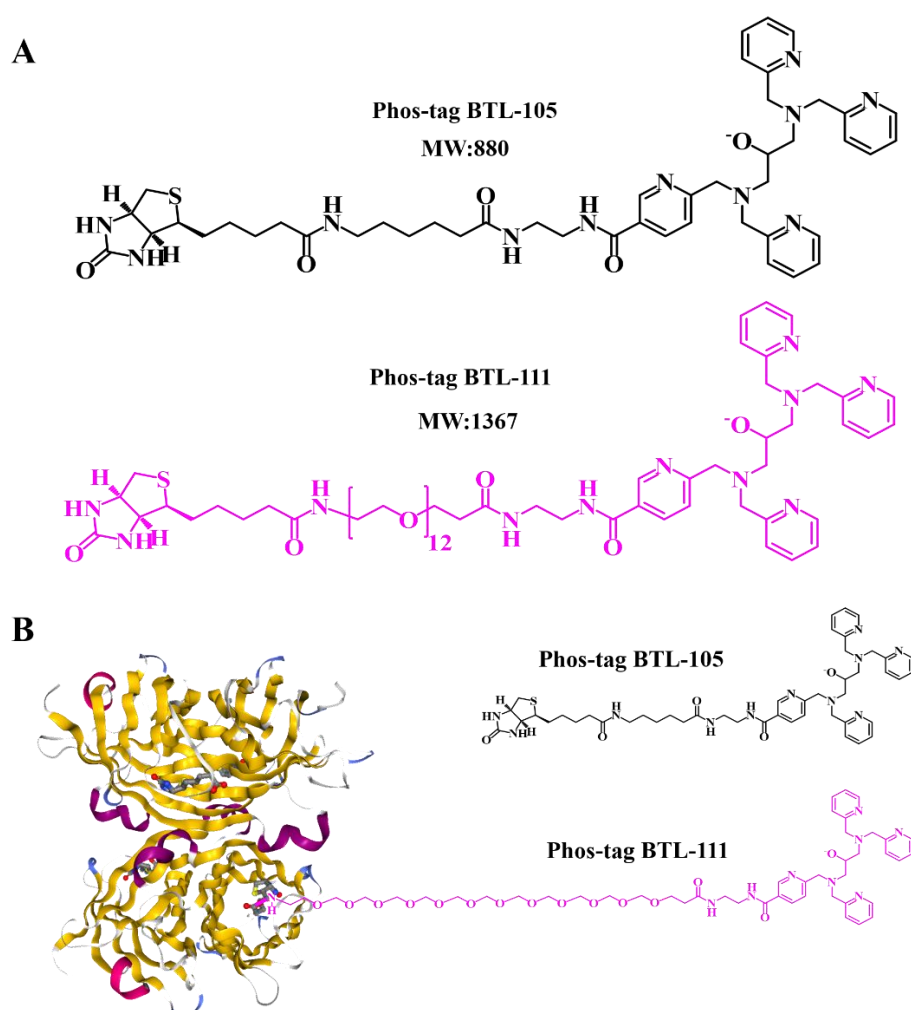


Fig. S9. (A) Chemical structure of phos-tag BTL-105 and phos-tag BTL-111. (B) Superimposed images of the complex of four biotin moieties, the tetrameric protein streptavidin, and the phos-tag BTL-111. The structure of the derivative BTL-105 is shown for reference.

7. Validation of different phos-tags

We evaluated the capability of different phos-tags (e.g., BTL-111 and BTL-105) for specific recognition of phosphate groups. In BTL-111, 12 molecules of ethylene glycol [PEG12; dodeca(ethylene glycol)] were inserted as a long hydrophilic spacer between a biotin moiety and a phos-tag moiety,³ while phos-tag BTL-105 contains only a spacer with five methylene molecules (Fig. S9A),⁴ and thus BTL-111 has a longer

hydrophilic spacer compared with BTL-105 (Fig. S9B). As shown in Fig. S10, the $F-F_0/F_0$ value in response to BTL-111 is much higher than that in response to BTL-105. This can be explained by the fact that the long hydrophilic spacer of BTL-111 confers a higher flexibility to the phos-tag molecule, making it more accessible to the phosphorylated peptides and proteins.⁴ Therefore, BTL-111 exhibits higher sensitivity and better specificity for the recognition of the phosphorylated peptides compared with BTL-105, and it is used in subsequent experiments.

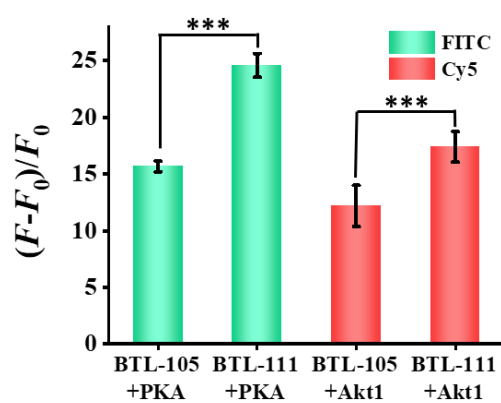


Fig. S10. Variance of the $F-F_0/F_0$ value with different phos-tag in the presence of PKA and Akt1, respectively. *** $p < 0.001$. Data are presented as means \pm SD (n = 3).

8. Optimization of the phos-tag concentration

The phos-tag is a specific phosphate-binding tag molecule that is the raw material for phosphoproteome research. The concentration of phos-tag may affect the detection sensitivity. Thus, the phos-tag concentration should be carefully optimized. We monitored the variance of the $F-F_0/F_0$ value with different concentrations of phos-tag (where F and F_0 are the fluorescence intensity in the presence and absence of protein kinase, respectively). As shown in Fig. S11, the $F-F_0/F_0$ value enhances with the

increasing concentration of phos-tag from 0.5 to 20 μM , and reaches a plateau beyond 20 μM . Therefore, 20 μM is selected for protein kinase assay in the following research.

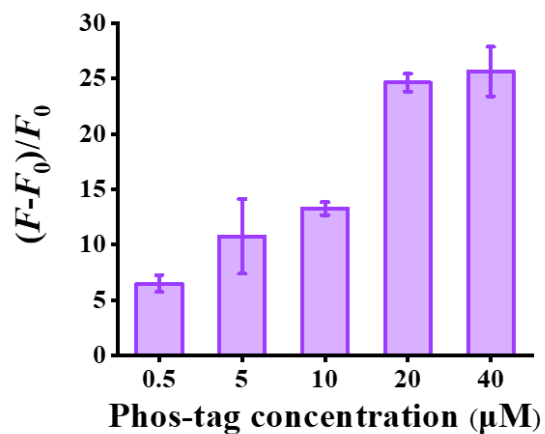


Fig. S11. Variance of $F-F_0/F_0$ value with the phos-tag concentration. Data are presented as means \pm SD (n = 3).

References

1. J. Gutenwik, B. Nilsson and A. Axelsson, *AIChE J.*, 2004, **50**, 3006-3018.
2. N. C. Stellwagen, *Electrophoresis*, 2009, **30 Suppl 1**, S188-195.
3. E. Kinoshita, E. Kinoshita-Kikuta, Y. Sugiyama, Y. Fukada, T. Ozeki and T. Koike, *Proteomics*, 2012, **12**, 932-937.
4. Z. He, Z. Wang, X. Nie, M. Qu, H. Zhao, X. Ji and Y. Wang, *Plant Physiol.*, 2022, **188**, 1385-1401.